Talanta 99 (2012) 262–269

Contents lists available at SciVerse ScienceDirect

Talanta

journal homepage: www.elsevier.com/locate/talanta

Characterization of diesel fuel by chemical separation combined with capillary gas chromatography (GC) isotope ratio mass spectrometry (IRMS)

Scott D. Harvey *, Kristin H. Jarman, James J. Moran, Christina M. Sorensen, Bob W. Wright

National Security Directorate, Pacific Northwest National Laboratory, Richland, WA 99352, United States

ARTICLE INFO

Article history:
Received 10 February 2012
Received in revised form
18 May 2012
Accepted 22 May 2012
Available online 29 May 2012

Keywords:
Differentiation of diesel fuel samples
Compound specific isotope analysis (CSIA) of diesel fuel *n*-alkanes
Hydrogen isotope ratio (δD) analysis
Carbon isotope ratio (δ^{13}C) analysis
Multi-element isotope ratio analysis
Principal components analysis (PCA)
Nearest neighbor classification of PCA scores

ABSTRACT

The purpose of this study was to perform a preliminary investigation of compound-specific isotope analysis (CSIA) of diesel fuels to evaluate whether the technique could distinguish diesel samples from different sources/locations. The ability to differentiate or correlate diesel samples could be valuable for discovering fuel tax evasion schemes or for environmental forensic studies. Two urea adduction-based techniques were used to isolate the *n*-alkanes from the fuel. Both carbon isotope ratio (δ^{13}C) and hydrogen isotope ratio (δD) values for the *n*-alkanes were then determined by CSIA in each sample. The samples investigated had δ^{13}C values that ranged from -30.1‰ to -26.8‰, whereas δD values ranged from -83‰ to -156‰. Plots of δD versus δ^{13}C with sample *n*-alkane points connected in order of increasing carbon number gave well-separated clusters with characteristic shapes for each sample. Principal components analysis (PCA) with δ^{13}C, δD, or combined δ^{13}C and δD data was applied to extract the maximum information content. PCA scores plots could clearly differentiate the samples, thereby demonstrating the potential of this approach for distinguishing (e.g., fingerprinting) fuel samples using δ^{13}C and δD values.

1. Introduction

The ability to determine unique chemical characteristics of a complex sample is critical for many applications. For petroleum-based materials, unique features aid in sample correlation and origin tracking and represent important applications in the geochemical and oil exploration areas. Likewise, the ability to track and identify sources for refined petroleum products, such as diesel fuel, also has important applications.

One application of uniquely identifying and tracking diesel fuel is to provide a scientific tool to discover fuel tax evasion. A number of possible schemes have been devised to evade payment of fuel tax. One dated source places the United States (U.S.) loss of tax revenue from fuel tax evasion at billions of dollars annually [1]. A number of potential U.S. fuel tax evasion schemes have been described [2]. For example, tax-free fuel reported as exported to a foreign destination may actually be sold domestically as taxed fuel with the evader keeping the tax revenue. Similarly, schemes that involve out-of-country sale with subsequent redelivery of the same fuel back to the U.S. as taxed fuel have been documented. Another scheme involves addition of non-taxed and/or lower value products (e.g., non-fuel petroleum products and waste streams such as used oils and solvents), products taxed at a lower rate (e.g., jet fuel), or unwanted petroleum products (e.g., high-sulfur diesel and refining intermediates) to the diesel fuel and selling the higher-volume blended or "cocktailed" mixture as taxed fuel, again with the evader keeping the tax revenue. Additional schemes include complex daisy chain paper trails that make it appear tax has been paid when in fact it has not. Numerous other fuel tax evasion schemes also exist, but are not described here [2].

Various chemical analysis techniques provide valuable tools for discovering fuel tax evasion. One important tool is high-resolution capillary gas chromatography which is used to create fuel fingerprints based on the compositional profile. These profiles, along with multivariate statistical analysis, can successfully allow sample correlation and determination of similar or common upstream distribution sources [3–6]. While this method allows reliable conclusions to be made, it can be difficult to differentiate fuels with very similar chromatographic profiles. It can also be problematic to determine if minor compositional changes arise from variation due to fuel source or from blending with other components or mixtures. Consequently, additional tools to complement and extend high-resolution, gas-chromatographic profiling techniques would be highly desirable. For instance, being able to fingerprint specific compounds in the chromatographic profile would add significant capability to discriminate unique sample attributes. In other words, using an orthogonal technique to "fingerprint the fingerprint" would provide enhanced capability.

* Corresponding author.
E-mail address: scott.harvey@pnnl.gov (S.D. Harvey).

0039-9140/$ - see front matter © 2012 Elsevier B.V. All rights reserved.
http://dx.doi.org/10.1016/j.talanta.2012.05.049

Isotope ratio mass spectrometry (IRMS) is another technique that has proven utility by characterizing unique isotopic features [7,8]. A broad range of applications for IRMS have been described, only a fraction of which deal with petroleum related topics [9]. Many of the petroleum-related studies focus on environmental forensics associated with spills and contamination or geochemical studies that address oil source and maturity [10]. Geochemical studies use IRMS extensively. Bulk analysis of crude oil (or compound class fractions that arise from group separations of crude oil) can help determine a sample's geochemical origins. Analysis of the bulk carbon isotope ratios ($\delta^{13}C$), along with GC profiling, can permit differentiation of different crude oil families [11], and augmentation by hydrogen isotope ratios (δD) can further enhance sample differentiation. The higher resolution made possible with δD analysis allows oil samples within families to be differentiated [12]. The combination of both $\delta^{13}C$ and δD determinations provides even higher sample discriminatory capability [7,12–17].

Compound-specific isotope analysis (CSIA) combines a separation technique (typically GC) with isotope measurement (often by IRMS) to determine isotope ratios of individual compounds within a mixed sample [18]. CSIA using multiple isotopes (i.e., both δD and $\delta^{13}C$) provides an additional dimension for sample fingerprinting [7,12]. In addition to organic isotope ratios, inorganic isotope determinations can be added to aid in origin determination [17]. Typically the $\delta^{13}C$ values for bulk petroleum fall within a limited range (~15‰) [7] and the values determined for individual *n*-alkanes extracted from a particular sample are fairly constant [19]. In contrast, δD values can encompass a wide range of values (~150‰) [12] and are observed to increase with increasing carbon number in the *n*-alkane series [12,20]. The compound-specific δD values can indicate whether a sample has a terrestrial or marine origin and, further, can differentiate among the terrestrial samples [21,22]. CSIA studies that determine both $\delta^{13}C$ and δD provide a detailed high-resolution fingerprint that can have enormous potential for determining sample origin. To our knowledge, only a handful of detailed CSIA publications have appeared that discuss both $\delta^{13}C$ and δD compound-specific data from petroleum samples [12,23]. Schimmelmann et al. analyzed samples by GC-IRMS for both δD and $\delta^{13}C$ and provided a plot of δD versus $\delta^{13}C$ values for the *n*-alkanes in a given sample, resulting in a sample fingerprint that allowed differentiating crude oil samples taken within the same geographical basin [12].

The motivation for this work was the development of an additional fingerprinting tool that can characterize unique diesel fuel features useful for sample correlations and source attribution. Specifically this work was aimed at distinguishing specific components within the complex diesel fuel profile for the purpose of detecting fuel tax evasion. This development is intended to complement and extend existing high-resolution gas-chromatographic fingerprinting approaches [3,6]. In practice, it is expected that CSIA would be applied as the secondary fingerprinting tool to very small sample sets (2–4 samples) after primary characterization using GC profiling. This study performs a preliminary evaluation of CSIA to see if the technique has value for distinguishing between diesel fuel samples that were collected at different times from diverse locations (presumably from different crude oils). Toward this end, the $\delta^{13}C$ and δD values for *n*-alkanes in each fuel sample were determined using two different chemical separation methods to isolate the *n*-alkane fraction followed by capillary gas chromatography (GC) combined with IRMS detection of numerous replicates for each of four diesel fuel samples. Novel aspects of this study include the combination of multi-isotope CSIA with multivariate statistical analysis to extract additional distinguishing information from diesel fuel samples.

2. Materials and methods

2.1. Chemicals

Anhydrous calcium chloride, nicotine, and urea were obtained from Sigma-Aldrich (Milwaulkee, WI, USA). Activated aluminum oxide (Brockmann I, 150 mesh, 58 Å) was also purchased from Sigma-Aldrich. PolyScience *n*-alkane standards were procured through Supelco (Bellefonte, PA). Carbon isotope measurements were corrected to an in-house *n*-octane standard (Acros, New Jersey, USA) which itself was calibrated using USGS40 (L-glutamic acid, $\delta^{13}C$ of −26.24‰) [24] and USGS41 (L-glutamic acid, $\delta^{13}C$ of +37.63‰) [25] obtained from the National Institute of Standards and Technology (Gaithersburg, MD, USA). *n*-Octane calibration was by elemental analysis coupled to IRMS. Hydrogen isotope measurements were calibrated using *n*-alkane (C_6–C_{30}) mix B2 (available from Indiana University Stable Isotope Reference Materials service, Bloomington, IN, USA). Methanol, pentane, and toluene solvents were purchased from Burdick & Jackson (Muskegon, MI, USA). The filters used during the urea adduction were 0.45-μm Phenex Nylon membranes from Phenomenex (Torrance, CA, USA).

2.2. Diesel samples

Four diesel fuel samples were investigated: R1409, R1410, R1411, and R1412. These samples were collected on the following dates from the locations indicated: (1) R1409 was collected in Myton, Utah on February 2011; (2) R1410 was collected in Kelso, Washington on October 2007; (3) R1411 was collected in New Jersey on November 2010; and (4) R1412 was collected in Orange, Texas during January 2008. Sample R1412 was a diesel/biofuel blend that contained 6.5% biodiesel by volume. From these different geographic locations and time periods, it is assumed that the crude oil from which the fuel was refined was likely sourced from different global locations.

2.3. n-Alkane isolation

Two different approaches were used to isolate the *n*-alkanes from diesel fuel. The first procedure isolated the aliphatic hydrocarbons by traditional column chromatography on activated alumina [26] followed by separating the aliphatic hydrocarbons into *n*-alkane and branched hydrocarbon fractions by urea adduction [27]. A diesel sample (3.0 mL) was applied to an alumina column (140 mm × 22 mm i.d.). The aliphatic hydrocarbons were eluted with 150 mL of pentane followed by elution of the aromatics with 200 mL of toluene. Urea adduction was performed on the aliphatic hydrocarbon fraction, as described by Lappas et al. [27], to separate the *n*-alkanes from the branched aliphatic hydrocarbons. Briefly, 1.2 mL of the aliphatic hydrocarbon fraction was added to a stirred slurry consisting of urea (3.0 g) and methanol (5.0 mL), and the urea clathrate complex was formed at progressively lower temperatures for prescribed times [27]. The solid urea adduct was then isolated by filtration (0.45 μm) and washed with pentane. *n*-Alkanes were isolated by dissolving the urea clathrate in 30 mL warm water, extracting three times with 7.0 mL of pentane, and drying the pentane with anhydrous calcium chloride. The composition of the aromatic, aliphatic hydrocarbon, *n*-alkane, and branched aliphatic hydrocarbon fractions was characterized by capillary GC and GC/MS analysis.

The second *n*-alkane isolation procedure involved two sequential applications of the urea adduction procedure applied directly on the diesel fuel, without first fractionating by column chromatography. The first urea adduction isolation was scaled up by a factor of 3 (i.e., 9.0 g urea and 15 mL methanol) to allow

processing of 3.0 g diesel fuel. Once the *n*-alkane fraction had been obtained, the urea adduction procedure (using 3.0 g of urea and 5.0 mL of methanol) was again applied in an attempt to further purify the *n*-alkanes. The first and second urea adduct fractions were analyzed by capillary GC/MS.

2.4. GC and GC/MS analysis

Diesel samples and fractions were analyzed on an Agilent Series 6890N gas chromatograph (Santa Clara, CA, USA) that contained either a flame ionization detector (FID) or an Agilent 5973 inert source mass-selective detector (MSD). Separations were performed with helium carrier gas on a 10 m × 100-μm i.d. column that contained a 0.17-μm film of DB-5 stationary phase (Agilent). Split injections (0.1 μL) were made into an injection port held at 250 °C with a split ratio of 400:1. The column was programmed from 60 °C to 280 °C at 20 °C/min after a 1 min post-injection hold, with a 3 min hold at 280 °C. The MSD collected full-scan mass spectra from 50 to 650 amu at a scan rate of 50 Hz. GC/MS analyses of the *n*-alkane fractions were also performed using the same column and conditions as were used for the CSIA as described below.

2.5. Compound-specific isotope analysis (CSIA)

Individual *n*-alkane components were isolated using a Thermo Trace GC Ultra gas chromatograph (Thermo Fisher, Waltham, MA, USA) fitted with a 60 m × 0.25 mm i.d. (d_f=0.25 μm) Rtx-1MS column (Restek, Bellefonte, PA, USA). *n*-Alkane samples were diluted 100-fold in hexanes prior to performing a split injection (2.5 μL, split ratio of 33:1) into a 290 °C injection port. Separations used a temperature program that started at 45 °C for 6 min, followed by a linear 10 °C/min ramp to a final temperature of 280 °C, with a 10 min hold at the final temperature. A Thermo Delta V Plus isotope ratio mass spectrometer (IRMS) was used for isotope measurements of eluting peaks. For carbon isotope determinations, the individual alkanes were converted to carbon dioxide and water using a micro-combustion reactor with a nickel, platinum, and copper catalyst held at 940 °C. Following water removal with a Nafion trap, the carbon dioxide passed through a Thermo GCC low-flow sample introduction system directly into the IRMS. For hydrogen isotope measurements, the hydrogen in the eluting *n*-alkane peaks was converted to molecular hydrogen using a ceramic microreactor coated with excess carbon and held at 1450 °C. All sample runs (for both carbon and hydrogen isotope measurements) employed multiple reference gas pulses before and after the sample peaks. For hydrogen measurements, the H_3^+ factor was calculated a minimum of once daily. Diesel chromatographic profiles obtained by CSIA paralleled those generated by GC-FID; high concentrations of *n*-alkanes were found at the chromatographic mid-range that decreased to low concentrations at the beginning and end of the chromatogram, as would be expected from a middle distillate cut. Isotope data is reported only for the peaks that fell within the linear concentration range (for carbon) or within the limits used for the H_3^+ factor determination (for hydrogen). A minimum of four replicates for carbon isotope determinations and eight replicates for hydrogen isotope measurements were performed on at least two different days. Standard deviations for all *n*-alkanes were ≤0.3‰ for carbon. The standard deviation for each *n*-alkane hydrogen analysis ranged from 2‰ to 11‰ with the average standard deviation being 4‰. The isotope ratio values are reported in delta (δ) notation where $\delta=[(R_{Sa}/R_{Std})-1]$, and R_{Sa} and R_{Std} are the isotope ratio ($^{13}C/^{12}C$ and $^{1}H/D$ for carbon and hydrogen analysis, respectively) of the sample and recognized international standards (Vienna Pee Dee Belemnite and Vienna Standard Mean Ocean Water for carbon and hydrogen, respectively).

2.6. Statistical analyses

Isotope ratio measurements (δD or δ^{13}C values) were plotted against the different samples for each individual *n*-alkane to summarize the data. One-way ANOVA followed by multiple comparisons tests were employed to determine significance of differences in *n*-alkanes between samples. Particularly, for both δD and δ^{13}C measurements, each *n*-alkane was tested by a one-way analysis of variance (ANOVA) across samples, followed by further examination using a multiple comparisons procedure to determine which sample pairs showed significant differences in isotope ratios. Differences at the $p<0.05$ level were deemed statistically significant, whereas differences at the $p<0.01$ level were considered highly significant.

Principal components analysis (PCA) was used to construct signatures of the complete δD or δ^{13}C *n*-alkane profile for the different samples. The PCA used *z*-scores, mean-centered and variance-normalized values, and plots of the loadings and scores were used to visualize differences between samples. Except as noted, all *n*-alkane δ^{13}C and δD values in the data set were measured above the concentration threshold required for precise IRMS determinations. Data analyses were conducted using the Matlab® R2011a software package.

3. Results and discussion

3.1. Isolation of n-alkanes

Diesel fuel is a complex distillate fraction that contains many thousands of compounds. Despite the high separation efficiencies achievable by capillary gas chromatography, capillary GC separations are still inadequate to ensure elution of pure components when analyzing highly complex mixtures [28]. Due to the isotopic heterogeneity within a chromatographic peak, CSIA requires baseline resolution between each component and any overlap between adjacent peaks compromises the ability to generate meaningful isotope values. This complicates isotopic determinations of individual components in complex mixtures because contaminants, along with their unique isotopic signatures, may be present in the chromatographic peaks. This situation is made worse by the extra-column band broadening associated with IRMS instrumentation that results in limited re-mixing of the chromatographically separated components. For this reason, the *n*-alkane fraction is isolated to simplify the sample to increase the probability of obtaining pure chromatographic peaks during the GC separation [29]. Once elution of a pure component is obtained, the IRMS data must be averaged over the entire peak to account for the earlier elution of isotopically heavier molecules (i.e., the chromatographic isotope effect). For isotopic δ^{13}C determinations, we investigated two isolation approaches to generate a purified *n*-alkane fraction for CSIA. Other *n*-alkane isolation methods based on adsorption using molecular sieve 5 A have been described but were not pursued in this work. Once the fractionation methodology was validated, one of the *n*-alkane isolation procedures was used for δD determinations.

Fig. 1(top) shows a high-resolution GC profile obtained on a 10 m × 100-μm i.d. capillary column of a representative diesel sample (R1409) used in this study. The complexity of the sample is readily apparent from the FID chromatographic trace. Numerous co-eluting components in the mixture result in a characteristic baseline "hump" in the chromatogram. To address the peak purity requirement for IRMS, this study isolated *n*-alkanes by either

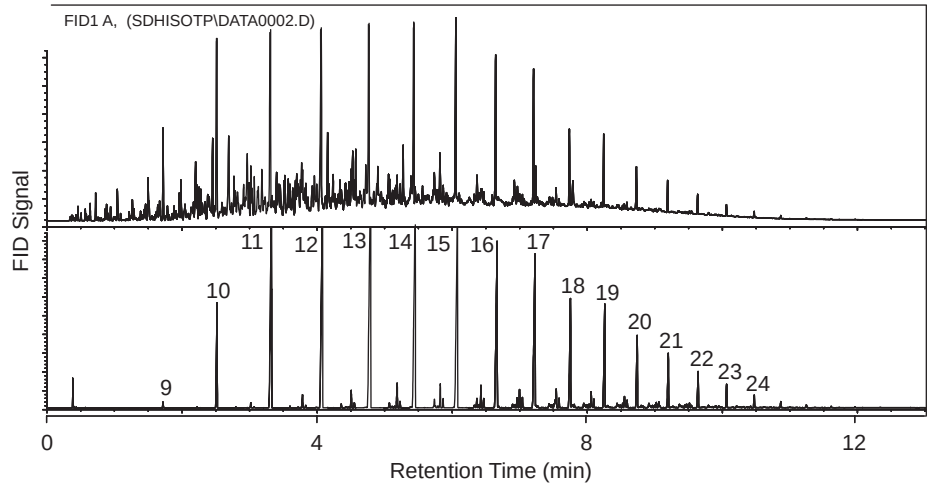

Fig. 1. High-resolution GC profiles of R1409 diesel fuel before (top) and after alumina fractionation and urea adduction to isolate the *n*-alkanes. A profile of the *n*-alkane fraction from R1409 is shown in the bottom chromatogram. The numbers refer to the number of carbons contained in the *n*-alkane.

column chromatography combined with urea adduction, or two successive urea adductions performed directly on the diesel fuel, to provide a relatively pure *n*-alkane fraction. Fig. 1(bottom) shows a chromatogram of the R1409 diesel fuel after isolating the *n*-alkanes by column chromatography followed by urea adduction. Chromatographic comparison shows that the separation was highly effective at removing interfering compounds. The GC profile features pure *n*-alkane peaks for *n*-C9–*n*-C28 with very little branched alkanes eluting between the peaks. GC-MS analysis of the purified *n*-alkane fraction identified the branched alkane contaminates that elute between the *n*-alkanes as 2- and 3-methyl branched alkanes, 3- and 4-alkyl branched alkanes, along with a variety of other alkyl substituents located near the terminus of the linear *n*-alkane chain.

GC analysis of the *n*-alkane fractionation obtained by column chromatography combined with urea adduction (Fig. 1, bottom) was nearly identical to the material isolated using two sequential urea adductions. Furthermore, GC analysis revealed there was very little difference between the *n*-alkane fractions resulting from the first and second urea adductions, suggesting that a single urea adduction performed directly on diesel fuel would be an adequate treatment prior to CSIA. An ANOVA conducted across sample preparation methodology revealed that the two *n*-alkane isolation methods gave statistically equivalent $\delta^{13}C$ values (2-tailed, $p > 0.05$), except for C_{12} in sample R1410 and C_{13} in sample R1412 that showed significant differences ($p < 0.05$). These results support the contention that there are few, if any, significant differences between the *n*-alkane profiles due to sample preparation. Therefore, for the GC-IRMS study described below, *n*-alkane fractions isolated by both methods were analyzed for $\delta^{13}C$, whereas δD measurements were performed on *n*-alkanes isolated by the column fractionation combined with the single urea adduction method. Only the results for the column chromatography combined with a single urea adduction method are presented here.

GC analysis of the diesel/biodiesel fuel blend (sample R1412) clearly showed the C16:0, C18:0, C18:1, and C18:2 fatty acid methyl esters (FAMES) eluting in between C_{19} and C_{22} *n*-alkanes in the diesel fuel profile. In fact, the C16:0 FAME elutes close to the C_{19} *n*-alkane, and the C18:2 FAME elutes immediately before a peak that contains both the C18:1 FAME and the C_{21} *n*-alkane. When the blended fuel was subjected to column chromatography followed by urea adduction, a FAME-free *n*-alkane fraction results that gives a similar purified *n*-alkane profile as shown in Fig. 1. The FAMES are retained on the alumina column and can be eluted separately with toluene or benzene. The double urea adduction, on the other hand, gave an *n*-alkane fraction that contained the FAMES. This indicates a limitation for the double urea adduction procedure when analyzing biodiesel-blended diesel fuels since chromatographic co-elution of FAMES with C_{19} and C_{21} often occurs. If blended fuels are suspected, and if isotopic determination of C_{19} and C_{21} *n*-alkane markers is deemed important, the column chromatography combined with urea adduction would be the preferred *n*-alkane isolation method.

3.2. CSIA of the n-alkane fraction

3.2.1. Injection-induced fractionation.

Previous studies have reported isotopic fractionation attributable to split GC injections, especially for volatile analytes injected using high split ratios [30,31]. We did not observe fractionation for acetone samples injected using a variety of split ratios that bracketed our analysis conditions. These data gave a mean of −157‰ with a standard deviation of 3‰ (relative standard deviation of 2%) for acetone δD values over the split ratio range from 4.4:1 to 33:1 ($N=30$). Furthermore, we tested for fractionation by comparing R1411-derived *n*-alkanes under splitless and split conditions and found no evidence for discrimination on our instrumentation under the analysis conditions used. Even if fractionation was observed, and it was not, only the accuracy of the more volatile *n*-alkanes should be influenced; relative sample comparisons would still be valid because samples would be affected in approximately the same way.

3.2.2. n-Alkane identification

To ensure that the *n*-alkanes were correctly identified during CSIA, traditional GC/MS was performed using the same column and chromatographic conditions. This provided mass spectral identification information for each *n*-alkane in the sample mixtures and gas-chromatographic retention time profiles that could be matched to the ion profiles obtained during CSIA.

3.2.3. $\delta^{13}C$ measurements

Fig. 2 presents $\delta^{13}C$ data for individual *n*-alkanes within each of the four diesel fuels. The figure shows the average $\delta^{13}C$ plotted against the number of carbons contained in the *n*-alkanes for each sample. Error bars representing one standard deviation from the average are provided for reference. Data are not shown for alkanes greater than C_{19} for sample R1409 or R1411 because the chromatographic peak intensities were below the threshold for precise

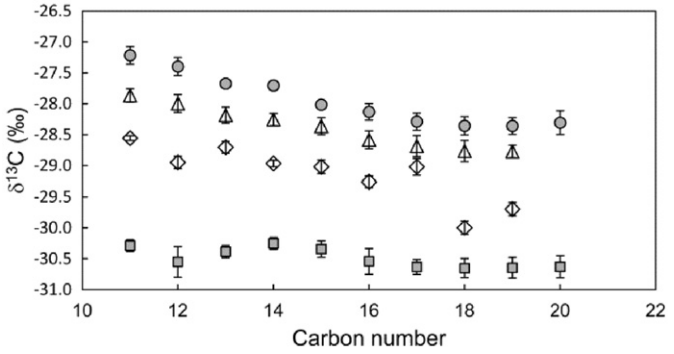

Fig. 2. Average δ^{13}C versus *n*-alkane carbon number for the four diesel fuels following column chromatography and a single urea adduct purification. Error bars shown are one standard deviation of replicate analyses for each *n*-alkane where analyses were performed in quadruplicate at a minimum. Samples include R1409 (-◇-), R1410 (-□-), R1411 (-△-), and R1412 (-○-).

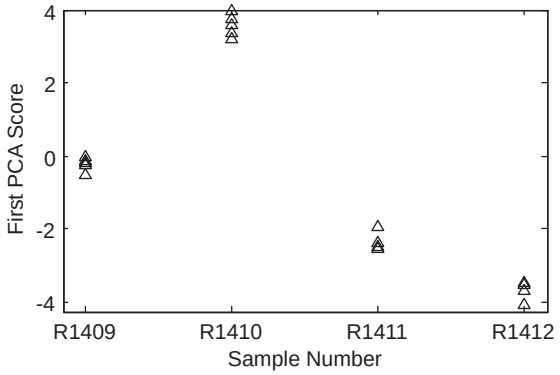

Fig. 3. First PCA score for the δ^{13}C *n*-alkane profile of diesel fuels as a function of sample number. Different score values for different types suggest that the C_{11}–C_{19} profiles are distinguishable from one another.

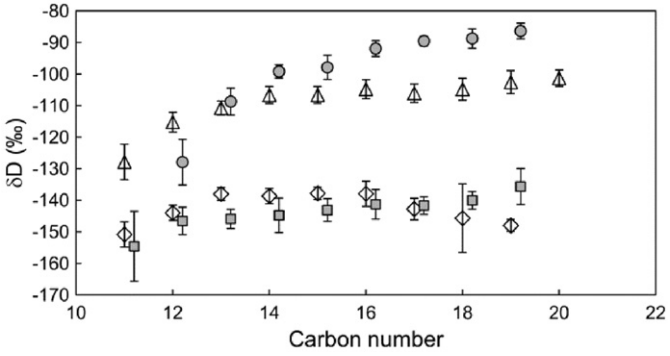

Fig. 4. Average δD versus *n*-alkane carbon number for the four diesel fuels following column chromatography and a single urea adduct purification. Error bars shown are one standard deviation of replicate analyses for each *n*-alkane where analyses were performed at a minimum of $n=8$. Note that the shaded symbols (correlating to data from samples R1410 and R1412) are reported with a 0.2 unit shift in carbon number to facilitate clear distinction of error bars. Samples include R1409 (-◇-), R1410 (-□-), R1411 (-△-), and R1412 (-○-).

isotopic determinations. The δ^{13}C range observed in the samples (from −26.7 to −30.2‰) is consistent with values reported in the literature for petroleum aliphatic hydrocarbons [7]. The δ^{13}C measurements indicate the isotope ratio drops with increasing alkane carbon number for all samples, except for R1410. Visually, sample R1410 stands out as being the most unique of the samples because it is more isotopically depleted and has a relatively flat δ^{13}C profile with increasing alkane carbon number. This is opposite of what would be expected from thermal cleavage or volatilization; these processes would result in smaller *n*-alkanes that are more isotopically depleted due to the kinetic isotope effect [12]. Investigators have observed both increasing [23] and decreasing δ^{13}C [21,27] with increasing *n*-alkane carbon number, depending on the oil sample being investigated. It has been suggested that the trend toward more isotopically depleted carbon with increasing carbon number, as observed in our study, may indicate significant algal or bacterial contributions to oil genesis [10,21,32].

Though the ANOVA results suggest that a single *n*-alkane could be used to differentiate samples, the problem becomes much more difficult in practice when there could be many different samples, some having similar δ^{13}C values for some of the alkanes and not others. Therefore, it is useful to combine all of the *n*-alkane values into a signature for a given fuel. Principal Component Analysis (PCA) was used for this purpose. The PCA revealed that 97.8% of the model variance could be described along the first principal component dimension. The C_{11}–C_{19} loadings for this first principal component were approximately equally weighted, ranging from −0.32 to −0.34, suggesting all of the *n*-alkanes are equally important in describing the variation between different samples. Furthermore, as Fig. 3 shows, examination of the scores shows obvious differences in the score values between different samples, suggesting distinctly different alkane profiles for the different fuels. To our knowledge, the CSIA of diesel fuel has not been described although previous work by Smallwood et al. [33] demonstrated that the majority of 19 gasoline samples could be differentiated based on δ^{13}C CSIA alone.

3.2.4. δD measurements

δD measurements have a high potential for differentiating samples due to the wide range of δD values found in petroleum samples [19]. Fig. 4 shows the plot of δD versus *n*-alkane carbon number for each diesel fuel sample. Data is not shown for alkanes greater than C_{19} for samples R1409, R1410, and R1412 because the chromatographic peak intensities were below the threshold for precise isotopic determinations. The δD values observed in this study range from −86‰ to −155‰ and are consistent with values described in the literature for petroleum [7]. With the exception of sample R1409, δD increases in each sample with increasing *n*-alkane carbon number. This increasing trend is by far the most predominant tendency that has been described in the literature for δD [10,12,20,34]. As previously described for δ^{13}C, a possible explanation for this trend in δD is based on bond strength. Carbon–carbon bonds that are adjacent to a C-D bond are stronger than those adjacent to C–H bonds. Thermal cracking will preferentially rupture the weaker carbon–carbon bonds resulting in more isotopically deficient smaller alkanes and, consequently, deuterium-enriched larger *n*-alkanes [12]. Sample R1409 displays a unique profile that initially increases and subsequently decreases at higher *n*-alkane carbon numbers. It is noteworthy that the samples presenting unique trends are different for δD (concave down for R1409) and δ^{13}C (flat profile for R1410). As with the δ^{13}C studies, δD plotted against increasing *n*-alkane carbon number give distinct sample fingerprints.

ANOVA for δD across samples suggests significant differences in the C_{12}–C_{19} *n*-alkanes. Subsequent multiple comparison analysis reveals significant differences in the mean C_{13}, C_{14}, C_{15}, and C_{19} values between any two sample pairs, indicating that the isotope ratios for these alkanes are distinct for each sample. For C_{12}, C_{16}, C_{17}, and C_{18}, there are significant differences overall, but the samples R1409 and R1410 are not statistically distinguishable,

nor are R1411 and R1412. Put another way, for C_{12}, C_{16}, C_{17}, and C_{18}, the mean δD values for R1409 and R1410 (or R1411 and R1412) are not significantly different, while the mean δD values for R1409 and R1411 or R1410 and R1412 are. Despite the similarities in specific alkanes between R1409 and R1410 (or R1411 and R1412), there remain *n*-alkanes that are significantly different between any two sample pairs.

As with the δ^{13}C data, signatures for each fuel type were constructed using PCA. Using *z*-scores of the δD values, PCA revealed that 97.2% of the variance could be described with the first principal component. The C_{12}–C_{19} loadings were approximately the same, varying between −0.35 and −0.36. As with the PCA of the δ^{13}C values, this suggests every alkane in the profile contributes to the variation between samples. As indicated in Fig. 5, the scores plot shows the similarities between R1409 and R1410 and between R1411 and R1412, along with the clear differences between the R1409/R1410 and R1411/R1412 sample pairs. These results suggest that while PCA of the δD profiles may be a useful tool for constructing profiles of different diesel fuel, these values are not, by themselves, sufficient to create unique signatures.

3.2.5. Combined δ^{13}C and δD measurements

Fig. 6 plots the average δD values versus δ^{13}C values for the *n*-alkanes in each of the four samples. Within a fuel, the *n*-alkane points are connected in order of increasing carbon number. The resulting line represents a high-resolution fingerprint that is unique for each sample. In relation to this work, Schimmelmann used similar plots to distinguish between oils collected within the same geographical basin [12]. The unique shapes of these curves could likewise allow differentiation and correlation among individual diesel fuel samples.

Given the similarity between δD profiles of different fuels and the large number of diverse fuels that will eventually be encountered in the practical application of this work, it may be useful to combine the δ^{13}C and δD measurements into an integrated signature, thereby maximizing the information content of the signature. To this end, a combined signature was constructed from the δ^{13}C and δD measurements by randomly pairing each δ^{13}C profile with a δD profile from the same sample. PCA was then performed on the *z*-scores of the combined data. This process was repeated several times with different randomizations, yielding results nearly identical to those presented in the following.

In the PCA, 91.1% of the variation is described in the first principal component, with an additional 7.4% of variation being provided for by the second principal component. The loadings of the first principal component are all approximately equal, ranging

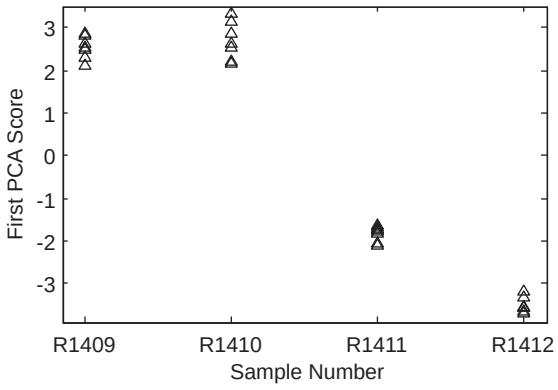

Fig. 5. First PCA score for the δD *n*-alkane profile of diesel fuels as a function of sample number. Similar score values for R1409 and R1410 suggest similar profiles. Different score values for the other sample pairs suggest their C_{12}–C_{19} profiles are distinguishable from one another.

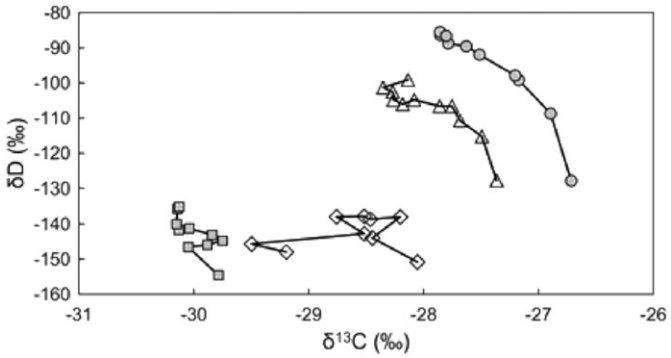

Fig. 6. δD versus δ^{13}C for the four diesel fuels. Each fuel presents a unique signature in this plot. Each sample has a line that sequentially connects hydrocarbons with increasing carbon number starting with the lowest *n*-alkane (value with the lowest δD value). Samples include R1409 (-◇-), R1410 (--□--), R1411 (-△-), and R1412 (--○--).

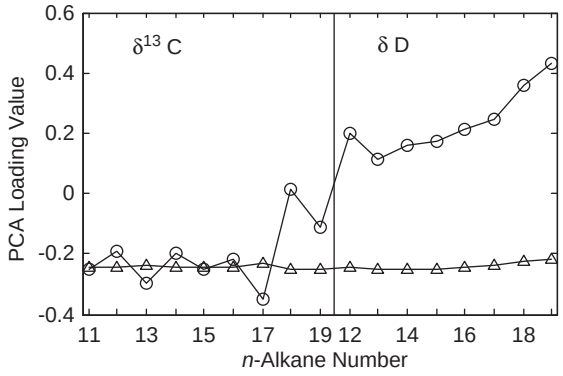

Fig. 7. First (-△-) and second (-○-) PCA loadings for the combined δ^{13}C and δD *n*-alkane profile of diesel fuels. *n*-Alkanes whose loading coefficients have a large magnitude tend to contribute most heavily to the sample-to-sample variation among the fuels.

from −0.25 to −0.22. The loadings of the second principal component range from −0.35 to 0.43, with the magnitude of the coefficient for only one measurement value, δ^{13}C C_{18}, falling below 0.1 (see Fig. 7). Similar to the loading values for the individual δD and δ^{13}C datasets, the first principal component indicates all *n*-alkanes are useful in describing the variation between fuel samples. With the exception of a few small coefficient values, the loadings of the second principal component tend to support this conclusion.

Fig. 8 plots the first and second PCA scores for the combined dataset. As expected, the different samples are well-separated from one another with respect to the within-sample variation.

Finally, to quantify how well different fuels might be distinguished from one another using a combined δD and δ^{13}C *n*-alkane profile, nearest neighbor classification of the PCA scores was performed on these data. Nearest neighbor classification is a procedure where a test sample is compared to a set of known-source samples, and associated with the group containing the nearest sample (the one with the smallest Euclidean distance in this study). Other, more sophisticated methods are available, however, the limited size of and preliminary nature of this dataset lends itself more to a simple method that doesn't require any statistical models rather than a more formalized approach.

In this work, each sample was treated as a test sample and its scores were compared to the scores of the remaining samples. It was then predicted as belonging to the fuel group of the nearest sample. Table 1 provides the results of this classification procedure. For each type of fuel, the number of correct and

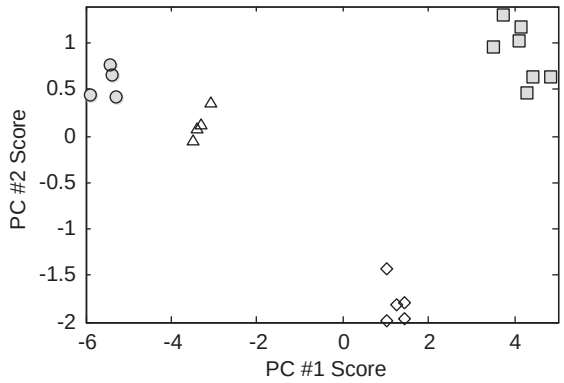

Fig. 8. First and second PCA scores for the combined δ^{13}C and δD *n*-alkane profile of diesel fuels, samples R1409 (-◇-), R1410 (-□-), R1411 (-△-), and R1412 (-○-). The clear separation between the different samples suggests these profiles may be useful for distinguishing diesel fuels from different sources.

Table 1
Classification results of combined δD and δ^{13}C *n*-alkane profiles for diesel fuel samples.

Fuel type	# Samples correctly classified	# Samples incorrectly classified
R1409	5	0
R1410	7	0
R1411	4	0
R1412	3	1 (classified as R1411)

incorrect classifications is reported. Only a single sample was misclassified, a R1412 sample. It was incorrectly classified as an R1411 sample. This near perfect classification provides further evidence that it is possible to differentiate diesel fuels based on their δD and δ^{13}C *n*-alkane profiles.

3.3. Future studies

The present study provides a proof-of-principle demonstration of multi-isotope CSIA for discriminating four different diesel fuels. Future studies should expand upon this work by conducting a blinded study that includes a more extensive sample base that also uses a large number of sample duplicates.

The results obtained suggest the chromatographic peak purity was adequate for CSIA, provided that the *n*-alkanes were first isolated from the diesel fuel. However, further chromatographic purification of the *n*-alkanes might be desirable to provide additional confidence in the peak purity. A recent advancement that could assist in further *n*-alkane purification is chromatography using a ZIF-8 stationary phase, a nanoparticulate zeolitic framework [35]. ZIF-8 has pores large enough to accommodate linear hydrocarbons, but not branched alkanes. Selective retention of *n*-alkanes on ZIF-8-coated capillary columns would allow repetitive collection of individual *n*-alkanes prior to analysis by CSIA. Alternatively, multidimensional GC × GC combined with IRMS detection [36–38] could be implemented using the ZIF-8 column for one dimension and an orthogonal non-polar column in the second dimension. Either approach would enhance confidence that pure alkane peaks are analyzed by CSIA.

4. Conclusions

These studies investigated CSIA as an analytical characterization technique that could complement high-resolution GC profiling to identify unique features in diesel fuel for sample correlation and differentiation. Such a tool would have value in discovering fuel tax evasion by providing orthogonal information on the similarity/differences between various fuel samples. This preliminary study examined four different diesel fuel samples, analyzing the δ^{13}C and δD *n*-alkane profiles for each sample, and constructing high-resolution isotope signature plots that showed little within-sample variation.

To meet the peak purity requirement for CSIA, diesel fuel was first fractionated to isolate the *n*-alkanes by two methods prior to GC separation. Both alumina chromatography followed by urea adduction and a double urea adduction procedure were highly effective in isolating the *n*-alkanes from diesel fuel; however, the FAMES are not completely removed from biodiesel blends by the double urea adduction. FAMES could potentially interfere with the determination of C_{19} and C_{21} *n*-alkanes, although our studies did not observe any obvious data distortion in the biodiesel blend data compared to the other diesel samples. Regardless, if biodiesel-blended fuel is being analyzed, it would be preferable to isolate the *n*-alkanes by normal-phase chromatography combined with urea adduction to remove the FAMES. An alternative method might involve *n*-alkane isolation using molecular sieve 5 A.

Isotopic ratio determinations for δ^{13}C followed by subsequent statistical analysis suggested that the C_{11}–C_{19} alkanes are useful in differentiating diesel fuels. In particular, ANOVA showed significant differences between the isotopics of different samples, and PCA plots showed clear groupings. δD values associated with different samples covered a much larger range than δ^{13}C and, therefore, have higher potential to offer even more discrimination. Nonetheless, many of the δD C_{12}–C_{19} isotopic ratios were determined to be significantly different between the different fuels, and PCA suggested distinct differences between the δD profiles (though not as distinct as the δ^{13}C profiles).

Given the promising results from the individual δ^{13}C and δD analyses, it is not surprising that the combination of both δ^{13}C and δD provided a clear indication of measurable differences between the different diesel fuels. Plots of δD versus δ^{13}C for *n*-alkanes in each sample show profiles that are well-separated from one another, and give characteristic shapes for each sample. PCA suggests nearly all of the δ^{13}C and δD isotope ratios contribute to the overall between-sample variation, and scores plots show clear groupings based on sample attributes.

This preliminary study shows that CSIA using multiple isotopes provides high-resolution analytical information with the potential to aid differentiation of diesel fuel samples. This approach may prove especially useful for distinguishing samples that have near-identical capillary GC profiles, or identifying waste components that have been added to the fuel. Pending studies to further develop this approach, the CSIA methodology along with statistical evaluation may provide a complementary tool to GC profiling for discovering fuel tax evasion. Clear extensions exist for additional petroleum distillate cuts, biodiesel, as well as other complex mixtures in general. On a more global view, the principles being developed are applicable for many studies where discrimination and correlation of complex samples are desirable.

Acknowledgments

This work was supported by the Internal Revenue Service (IRS) under an Interagency Agreement with the U.S. Department of Energy (DOE) under Contract DE-AC05-76RLO1830. The views, opinions, and findings contained within this paper are those of the authors and should not be construed as an official position, policy, or decision of the DOE or IRS unless designated by other documentation. The authors gratefully acknowledge the GC

support provided by Tucker D. Gilman and the GC/MS support provided by Richard B. Lucke.

Appendix A. Supplementary data

The $\delta^{13}C$ and δD values determined during this study, along with their averages and standard deviations, are presented in the supplementary data section.

Supplementary data associated with this article can be found in the online version at http://dx.doi.org/10.1016/j.talanta.2012.05.049.

References

[1] S.J. Baluch, Transp. Res. Rec. 1558 (1996) 67–73.
[2] M.E. Peters, Statement of Mary E. Peters, Administrator Federal Highway Administration, Before the Committee on Finance, United States Senate. Hearing on Schemes, Scams, and Cons: Fuel Tax Fraud, U.S. Department of Transportation, Washington, DC, 2002, July 17.
[3] K.M. Pierce, J.L. Hope, K.J. Johnson, B.W. Wright, R.E. Synovec, J. Chromatogr. A 1069 (2005) 101–110.
[4] S.A. Stout, A.D. Uhler, K.J. McCarthy, S.D. Emsbo-Mattingly, in: B.L. Murphy, R.D. Morrison (Eds.), Introduction to Environmental Forensics, Academic Press, Boston, 2002, pp. 137–260.
[5] R.M. Uhler, E.M. Healey, K.J. McCarthy, A.D. Uhler, S.A. Stout, Int. J. Environ. Anal. Chem. 83 (2003) 1–20.
[6] K.L. Johnson, B.W. Wright, K.H. Jarman, R.E. Synovec, J. Chromatogr. A 996 (2003) 141–155.
[7] S. Benson, C. Lennard, P. Maynard, C. Roux, Forensic Sci. Int. 157 (2006) 1–22.
[8] J.R. Ehleringer, T.E. Cerling, J.B. West, in: R.D. Blackledge (Ed.), Forensic Analysis on the Cutting Edge: New Methods for Trace Evidence Analysis, Wiley, New York, 2007, pp. 399–422.
[9] W. Meier-Augenstein, J. Chromatogr. A 842 (1999) 351–371.
[10] M. Asif, K. Grice, T. Fezeelat, Org. Geochem. 40 (2009) 301–311.
[11] K.R. Al-Arouri, D.M. McKirdy, C.J. Boreham, Org. Geochem. 29 (1998) 713–734.
[12] A. Schimmelmann, A.L. Sessions, C.J. Boreham, D.S. Edwards, G.A. Logan, S.E. Summons, Org. Geochem. 35 (2004) 1169–1195.
[13] W. Meier-Augenstein, R.H. Liu, in: J. Yinon (Ed.), Advances in Forensic Application of Mass Spectrometry, CRC Press, Boca Raton, 2003, pp. 149–180.
[14] N. Turner, M. Jones, K. Grice, D. Dawson, M. Ioppolo-Armanios, S.J. Fisher, Atmos. Environ. 40 (2006) 3381–3388.
[15] T.S. Pilgrim, R.J. Watling, K. Grice, Food Chem. 118 (2010) 921–926.
[16] C.V. von Eckstaedt, K. Grice, M. Ioppolo-Armanios, M. Jones, Atmos. Environ. 45 (2011) 5477–5483.
[17] C.V. von Eckstaedt, K. Grice, M. Ioppolo-Armanios, G. Chidlow, M. Jones, J. Chromatogr. A 1218 (2011) 6511–6517.
[18] A.L. Sessions, J. Sep. Sci. 29 (2006) 1946–1961.
[19] M. Li, Y. Huang, M. Obermajer, C. Jiang, L.R. Snowdon, M.G. Fowler, Org. Geochem. 32 (2001) 1387–1399.
[20] N. Pedentchouk, K.H. Freeman, N.B. Harris, Geochim. Cosmochim. Acta 70 (2006) 2063–2072.
[21] J.E. Cortes, J.M. Rincon, J.M. Jaramillo, R.P. Philp, J. Allen, J. South Am. Earth Sci. 29 (2010) 198–213.
[22] J.M. Hunt, R.P. Philp, K.A. Kvenvolden, Org. Geochem. 33 (2002) 1025–1052.
[23] D. Dawson, K. Grice, R. Alexander, D. Edwards, Org. Geochem. 38 (2007) 1015–1038.
[24] T.B. Coplen, W.A. Brand, M. Gehre, M. Gröning, H.A.J. Meijer, B. Toman, R.M. Verkouteren, Anal. Chem. 78 (2006) 2439–2441.
[25] H. Qi, T.B. Coplen, H. Geilmann, W.A. Brand, J.K. Böhlke, Rapid Commun. Mass Spectrom. 17 (2003) 2483–2487.
[26] A.A. Lappas, D.T. Patiaka, B.D. Dimitriadis, I.A. Vasalos, Appl. Catal. A 152 (1997) 7–26.
[27] A.A. Lappas, D. Patiaka, D. Ikonomou, I.A. Vasalos, Ind. Eng. Chem. Res. 36 (1997) 3110–3115.
[28] J.C. Giddings, in: H.J. Cortes (Ed.), Multidimensional Chromatography, Techniques and Applications, Marcel Dekker, New York, 1990, pp. 1–27.
[29] L. Ellis, A.L. Fincannon, Org. Geochem. 29 (1998) 1101–1117.
[30] J. Schmitt, B. Glaser, W. Zech, Rapid Commun. Mass. Spectrom. 17 (2003) 970–977.
[31] W. Meier-Augenstein, J. Chromatogr. A 752 (1996) 1996.
[32] A.P. Murray, R.E. Summons, C.J. Boreham, L.M. Dowling, Org. Geochem. 22 (1994) 521–542.
[33] B.J. Smallwood, R.P. Philp, J.D. Allen, Org. Geochem. 33 (2002) 149–159.
[34] K.L. Pond, Y. Huang, Y. Wang, C.F. Kulpa, Environ. Sci. Technol. 36 (2002) 724–728.
[35] N. Chang, Z.-Y. Gu, X.-P. Yan, J. Am. Chem. Soc. 132 (2010) 13645–13647.
[36] H.J. Tobias, G.L. Sacks, Y. Zhang, J.T. Brenna, Anal. Chem. 80 (2008) 8613–8621.
[37] S. Nitz, B. Weinreich, F. Drawert, J. High Resolution Chromatogr. 15 (1992) 387–391.
[38] D. Juchelka, T. Beck, U. Hener, F. Dettmar, A. Mosandl, J. High Resolution Chromatogr. 21 (1998) 145–151.